

# SPARSE TARGET RECOVERY PERFORMANCE OF MULTI-FREQUENCY CHIRP WAVEFORMS

*Emre Ertin, Lee C. Potter, and Randolph L. Moses*

Department of Electrical and Computer Engineering  
The Ohio State University  
Columbus, Ohio  
ertin.1@osu.edu

## ABSTRACT

Imaging radars employ wideband linear frequency modulation (LFM) waveforms to achieve high resolution while maintaining moderate sampling rates through restricting the target support to a known range interval and using stretch (deramp) processing. In recent work motivated by compressive sensing principles, multi-frequency extensions of the chirp waveforms were proposed to obtain randomized projections of range profiles. This paper considers the sparse target recovery problem with chirp transmit waveforms and their multi-frequency extensions. We derive the sensing matrix for multi-frequency chirp waveforms and study its coherence properties. We show that multi-frequency chirp waveforms result in sensing matrices with lower coherence between the columns resulting in improved target estimation performance compared to the standard LFM waveform.

## 1. INTRODUCTION

Radar sensors extract information about the targets in its range by transmitting bandpass RF waveforms to probe the target channel and sampling the backscatter return after suitable receive filtering. Imaging sensors achieve high resolution using wideband modulated waveforms and match filtering on receive [10]. Digital implementation of match filtering requires sampling of the received waveforms at the Nyquist rate of the transmit waveform. For the special case of chirp waveforms with linear frequency modulation the match filtering can be implemented through a combination of analog mixing stage and sampling at a fraction of the Nyquist rate proportional to the ratio of the target spatial support to the pulse width. In recent work [6], motivated by compressive sensing principles [3, 2], Ertin proposed the use of multi-frequency extension of chirp processing chain termed as compressive illumination to obtain randomized projections of the range profile.

In this paper we study sparse recovery performance of compressive illumination strategies. We first model radar imaging as a channel sensing problem where the channel impulse response is estimated from its noisy linear projections. Next we derive the sensing matrix for single and multi-frequency chirp transmit waveforms and provide a brief review of results from the literature relating stable recovery of sparse signals to the coherency of the sensing matrix. We show that compressive illumination with multi-frequency chirp waveforms with appropriate received processing results in lower coherence sensing matrices and improved target support recovery performance as compared to traditional single carrier chirp signaling.

## 1.1 Sensing Matrices for Radar Imaging

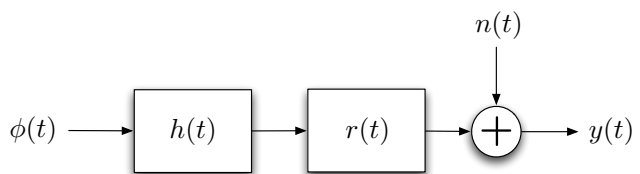


Figure 1: Radar as a channel sensing problem

Figure 1 shows the radar sensing model. The radar sensor transmits a waveform  $\phi(t)$  which is convolved by the target channel response  $h(t)$  and then filtered by the receive filter  $r(t)$  and sampled. We assume the waveform  $\phi(t)$  is the complex baseband form of the transmitted waveform with finite energy  $E$  over the pulse length  $[0, \tau]$ :

$$E = \int_0^\tau |\phi(t)|^2 dt \quad (1)$$

We assume the complex baseband target response  $h(t)$  is a random process that models a causal impulse response of a linear time invariant system with known support  $[\frac{-R_r}{c}, \frac{R_r}{c}]$  in time. The noise waveform  $n(t)$  is a Gaussian random process with known constant power density, bandlimited to receiver bandwidth.

Discretization of the sensing model results in the vector model given in Equation (2), where the  $M \times 1$  measurement vector  $y$  is a noise-corrupted version of the transmitted waveform  $\phi$  that has propagated through a sequence of two linear operators: target channel filter  $H$  and receiver shaping filter  $R$ .

$$y = RH\phi + n \quad (2)$$

The convolution matrix  $H$  is formed using the unknown target response, whereas the receive filter convolution matrix  $R$  is formed using the known filter impulse response  $r(t)$ . The vector  $n$  represents sensor output noise with complex circularly symmetric additive white Gaussian noise with known variance  $\sigma_n$ . The model in (2) can be extended to incorporate multiple transmitters and/or receivers, and time-varying channels and receive and transmit operations. In this paper we consider a static scene and time-invariant filter operation and a single coherent pulse. Multiple pulses can be easily incorporated in the model by concatenating outputs from different pulses increasing the length of the received signal vector and the transmit waveform vector.

Linearity of the channel operator  $H$  enables us to write the channel output vector  $H\phi$  equivalently as  $\Phi h$ , where  $h$  is an  $N \times 1$  vector of channel impulse response  $h(t)$ , and  $\Phi$  is a linear operator appropriately constructed from  $\phi$ . This results in:

$$y = R\Phi h + n \quad (3)$$

In addition we consider target responses with a sparse representation in some given basis  $\Psi$  (i.e.,  $h = \Psi x$  for sparse  $x$ ), resulting in the standard sparse sensing model:

$$y = Ax + n \quad (4)$$

where the  $M \times N$  matrix  $A(\Phi, R) \triangleq R\Phi(\phi)\Psi$  serves as the sensing matrix of the radar system,  $rxop$  is the convolution matrix with transmit waveform  $\phi(t)$ ,  $\Phi$  is the convolution matrix of the receive filter  $r(t)$ . In the remaining of the paper we will assume that the target scene consists of small number of point scatterers, or equivalently that the discretized target impulse response itself is sparse (i.e.  $\Psi = I$ ).

## 1.2 Sparse Signal Recovery and Mutual Coherence

Compressed sensing research considers the linear inverse problem given in Equation (4), which is recovery of a signal  $x$  from noisy measurements of its linear projections. The focus is on the underdetermined problem where the sensing matrix  $A$  forms a non-complete basis with  $M < N$ . The resulting ill-posed inverse problem is regularized assuming:

- (a) that the unknown signal  $x$  has at most  $K$  non-zero entries
- (b) the noise process is bounded by  $\|n\|_2 < \varepsilon$ .

Results in CS theory provides sufficient conditions for stable inversion of the forward problem given in (4) for a class of forward operators  $A$ . One such class of operators is defined through a bound on the singular values of the submatrices of  $A$ . Specifically, the restricted isometry constant (RIC)  $\delta_s$  for forward operator  $A$  is defined as the smallest  $\delta \in (0, 1)$  such that:

$$(1 - \delta_s)\|x\|_2^2 \leq \|Ax\|_2^2 \leq (1 + \delta_s)\|x\|_2^2 \quad (5)$$

holds for all vectors  $x$  with at most  $s$  non-zero entries. One sufficient condition in the literature shows that for forward operators with suitably small restricted isometry constant ( $\delta_{2K} < \sqrt{2} - 1$ ), stable signal recovery of  $K$ -sparse signals can be achieved through the solution of the computationally tractable  $\ell_1$  regularized inverse problem [1] termed as Basis Pursuit:

$$\min_x \|x\|_1 \text{ subject to } \|Ax - y\|_2^2 \leq \varepsilon. \quad (6)$$

In effect, the convex optimization problem in (6) approximates the solution for the NP-hard problem of finding the sparsest feasible solution given below in (7) with bounded error.

$$\min_x \|x\|_0 \text{ subject to } \|Ax - y\|_2^2 \leq \varepsilon, \quad (7)$$

where  $\|\cdot\|_0$  is the  $\ell_0$  semi-norm, i.e. the number of nonzero entries in the vector. For large  $M$ , estimating and testing the restricted isometry constant is impractical. A computationally efficient, yet conservative bound on RIC can be obtained through the *mutual coherence* of the columns of  $A$  defined as:

$$\mu(A) = \max_{i \neq j} \frac{|A_i^H A_j|}{\|A_i\| \|A_j\|}. \quad (8)$$

An equivalent definition of mutual coherence is the maximum of the absolute of the off-diagonal entries of the Gram Matrix  $G = \tilde{A}'\tilde{A}$ , where  $(\cdot)'$  denotes the Hermitian transpose and  $\tilde{A}$  is computed through normalizing columns of  $A$  to have unit norm:

$$\mu(A) = \max_{i \neq j} |G_{ij}| \quad (9)$$

Mutual coherence can be used to guarantee stable inversion through  $\ell_1$  recovery (6), since RIC is bounded by  $\delta_s < (s - 1)\mu$ . The bounds based on the maximal element of the off-diagonal entries of the Gram matrix (mutual coherence) are often quite pessimistic in practice which led the study of alternative metrics for sensing matrix optimization based on average measures of coherence.

Tropp [11] used cumulative coherence function  $\mu(m; A)$  defined for each natural number  $m$  as:

$$\mu(m; A) = \max_{|\Lambda| < m} \max_{j \notin \Lambda} \sum_{i \in \Lambda} |G_{ij}|. \quad (10)$$

to bound the performance of convex relaxation of the sparse recovery problem. Elad [5] proposed  $t$ -averaged mutual coherence metric defined as:

$$\mu_t(A) = \frac{\sum_{i \neq j} (|G_{ij}| > t) \cdot |G_{ij}|}{\sum_{i \neq j} |G_{ij}| > t} \quad (11)$$

Elad fixes a target value for  $t$  and optimize the sensing matrix  $A$  to iteratively minimize  $\mu_t(A)$ . An alternative direct strategy proposed by Duarte-Carvajalino *et al.* [4] attempts to design the sensing matrix to make the associated Gram matrix as close as possible to the identity matrix.

In the following we derive the sensing matrix  $A$  for multi-frequency chirp waveforms and study the coherence of the columns of  $A$  and show that the proportion of large values in the off-diagonal entries of the Gram matrix is significantly reduced as compared to the traditional single frequency chirp waveform suggesting better sparse target recovery performance. Through simulation experiments we verify improved MSE performance of radar sensors with compressive illumination for various values of sparsity  $\delta = K/N$  and signal-to-noise (SNR) ratio.

## 2. SENSING MATRICES FOR MULTI-FREQUENCY CHIRP WAVEFORMS

In this section we derive the sensing matrix of a multi-frequency linear FM waveform with staggered carrier frequencies and study its coherence distribution empirically. The time-domain waveform for  $K$  sub-carriers is given by:

$$f(t) = \sum_{k=1}^K e^{j\phi^k} \text{rect}\left(\frac{t}{\tau}\right) \exp\left(j2\pi\left(f^k t + \frac{\alpha}{2} t^2\right)\right) \quad (12)$$

where  $\alpha$  is the common chirp-rate,  $\tau$  is the pulse width,  $f^k$  and  $\phi^k$  is the frequency and the complex phase of the  $k$ 'th carrier. The bandwidth  $B$  of each linear frequency waveform is equal and is given by  $B = \tau\alpha$ . The backscatter return from a target at range  $d$  will result in two-way time delay of  $t_d = \frac{2d}{c}$ . Without loss of generality we can assume that the frequency of the first carrier is fixed at  $f^1 = f_0$ , where  $f_0$  is

the frequency of the reference carrier used at the receiver for dechirping.

$$r(t) = c \sum_{k=1}^K e^{j\phi^k} \text{rect}\left(\frac{t-t_d}{\tau}\right) \times \exp\left(j2\pi(f^k(t-t_d) + \frac{\alpha}{2}(t-t_d)^2)\right) \quad (13)$$

The amplitude  $c$  of the return signal depends on the target radar cross section, propagation delay and overall radar system gain. The return signal is dechirped with a reference linear frequency waveform of fixed carrier frequency  $f_0$ :

$$m(t) = \text{rect}\left(\frac{t-t_r}{\tau_r}\right) \exp\left(-j2\pi(f_0 t + \frac{\alpha}{2}t^2)\right) \quad (14)$$

The receive window  $\tau_r$  and the reference range delay  $t_r$  is determined by the unambiguous range  $R_u = R_{max} - R_{min}$  and the reference range  $R_r = (R_{max} + R_{min})/2$  through:

$$\tau_r = \frac{2R_u}{c} \quad t_r = \frac{2R_r}{c}. \quad (15)$$

The resulting wideband signal  $s(t) = m(t)r(t)$  at the input of the low-rate A/D is given by:

$$s(t) = c \sum_{k=1}^K e^{j\phi^k} \text{rect}\left(\frac{t-(t_d-t_r)}{\tau}\right) \times \exp\left(j2\pi((f^k - f_0)t - f^k t_d)\right) \times \exp\left(j2\pi(-\alpha t t_d + \frac{\alpha}{2}t_d^2)\right) \quad (16)$$

Collecting significant terms, we can simplify equation (16) further as:

$$s(t) = c \sum_{k=1}^K e^{j\phi(f^k, t_d, \phi^k)} \text{rect}\left(\frac{t-(t_d-t_r)}{\tau}\right) \times \exp\left(j2\pi((f^k - f_0 - \alpha t_d)t)\right) \quad (17)$$

where the overall phase of the signal  $\phi(f^k, t_d, \phi^k)$  is given by:

$$\phi(f^k, t_d, \phi^k) = \phi^k - 2\pi f^k t_d \quad (18)$$

We observe that the resulting signal is composed of multiple sinusoids whose instantaneous frequency is given by:

$$f_{inst} = (f^k - f_0 - \alpha t_d) \quad (19)$$

Now, the compressive measurement is obtained by using an A/D with a low sampling rate of  $f_s = 2\alpha\tau_r$ . this results in aliasing of the multiple sinusoids in to the baseband  $[-f_s/2, f_s/2]$  with random complex coefficients given in Equation (18) and frequency components given in Equation (19).

If we consider the discretized version of the unknown range profile as the vector  $x$ , with range bins at  $d_k = k\Delta$  then the time domain measurement vector  $y$  at the output of the A/D can be modeled as

$$y = Ax + n \quad (20)$$

where column  $k$  of the sensing matrix  $A$  correspond to FFT of the samples given in Equation (17) for a singular target vector at range bin  $k$  corresponding to a delay of  $t_d = 2(R_{min} - k\Delta)/c$ . Figure 2 shows a single column of  $A$  for a chirp waveform modulated by 10 subcarriers. As a result 10 copies of the single target is aliased into the baseband at known locations corresponding to the carrier differences  $f^k - f_0$ . We note that targets that are closer than the reference range  $R_r$  appears at negative relative range. In the following section we study the coherence of the columns of the sensing matrix  $A$  and study sparse target recovery performance empirically through simulations.

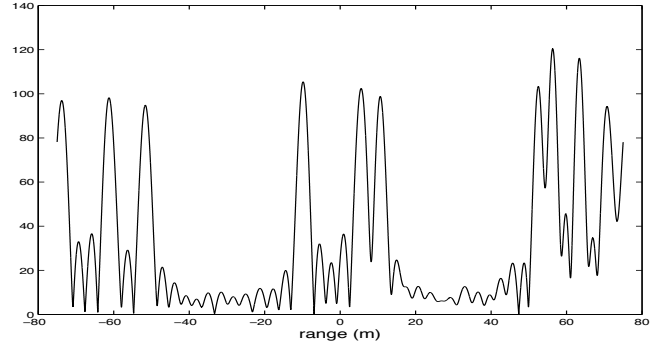


Figure 2: Sampled returns for a compressive illumination radar receiver

The concept of using low-resolution radar receivers at different frequencies have been proposed before. Gjessing [7] considers use of multi-frequency continuous wave radar system for high range resolution radar applications, Jankiraman [8] describes a wideband radar system with multi-frequency linear FM continuous transmit waves and matching number of stretch processors. The compressive illumination technique studied in this paper relies on purposefully aliasing multiple copies of the target response with known pattern with the goal of maximizing the information rate of low-frequency A/Ds. The block diagram of the compressive illumination sensor is given in Figure 3. Specifically, the radar system transmits a multi carrier LFM signal and the received signals from the multiple carriers are aliased onto the narrowband receiver of a single carrier requiring only a slower A/D. The design complexity is not dependent on the number of carriers. We note that the aliasing in range strategy through transmitter diversity is similar in spirit to Mishali and Eldar's [9] work on aliasing across the frequency domain for signals with sparse bandwidth support, where the aliasing projections are implemented in the receiver.

### 3. COHERENCY DISTRIBUTION OF RADAR SENSING MATRICES

As discussed in Section 1.2, minimizing large entries of the off-diagonal entries of the Gram matrix is essential for stable recovery of a sparse signal from its noisy projections. We consider the empirical cumulative distribution function  $F(t; A)$  of the entries of the Gram matrix derived from  $A$ :

$$F(t; A) = \frac{\sum_{i>j} (G_{ij} > t)}{N(N-1)/2}. \quad (21)$$

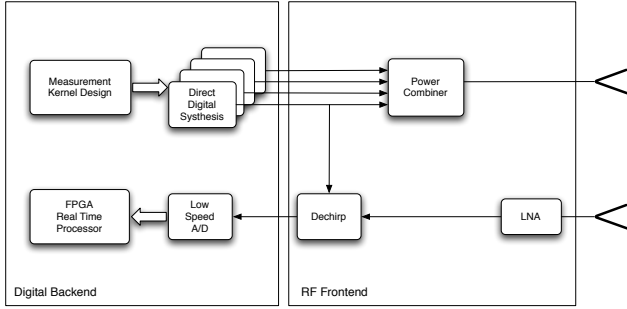


Figure 3: Block Diagram of the Radar Sensor with Compressive Illumination

Figure 4 shows  $F(t;A)$  for multi-frequency chirp transmit waveform with  $M = 1, 7, 15$  subcarriers. We observe that the percentage of entries exceeding a small threshold of  $t = 0.5$  is significantly higher for the traditional single carrier waveform suggesting a higher percentage of target realizations will result in poor recovery with a standard LFM radar with  $M = 1$  carrier.

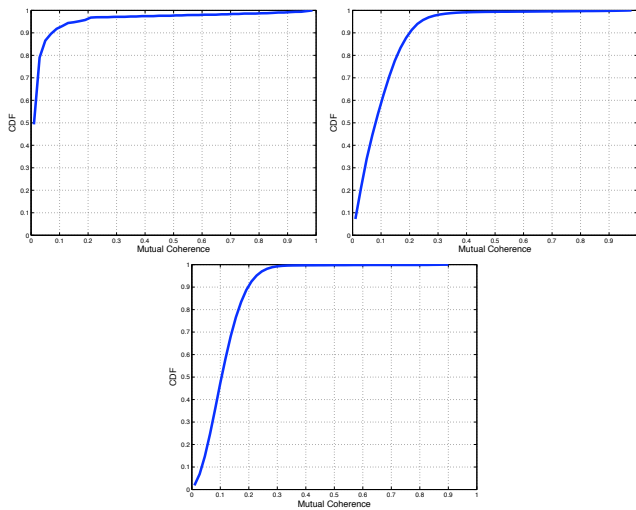


Figure 4: Empirical cumulative distribution of the off-diagonal entries of the gram matrix  $G$  for transmit waveform with  $M = 1, 7, 15$  subcarriers

Next, for an empirical verification of this insight we report simulation results that characterize MSE performance of sparse target estimation through the Basis Pursuit algorithm.

#### 4. SIMULATION STUDY OF SPARSE TARGET RECOVERY PERFORMANCE

In this section we present results of a Monte Carlo simulation study of multi-frequency chirp transmit waveforms combined with a deramp receiver whose output is sampled using a low rate A/D. The simulations are conducted over different number of subcarriers ( $M = 1, 7, 15$ ), target sparsity levels ( $\delta = K/N$ ) ranging from 0.1 to 1 and SNR levels ranging from 0 to 60dB. For each  $M, \delta, SNR$  simulation step, 100 Monte Carlo realizations have been used. We simulated multi-frequency linear FM signals with 750 MHz total bandwidth and 10  $\mu$ second duration, composed of  $M$  subcarri-

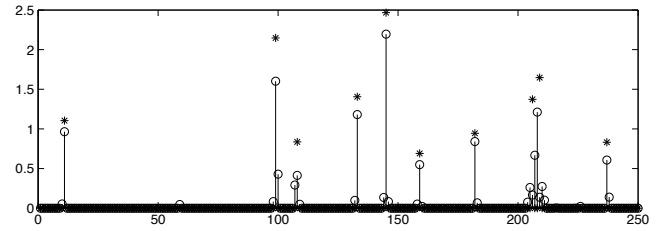
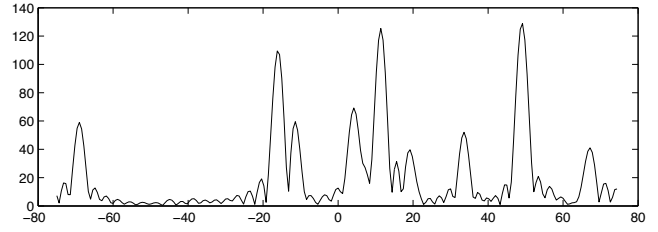


Figure 5: (Top) Received signal for a single carrier transmit LFM waveform and dechirp receiver, (Bottom) Sparse Recovery of target response using BP, \* shows the true target locations and amplitudes,  $\circ$  shows the detected target locations and amplitudes

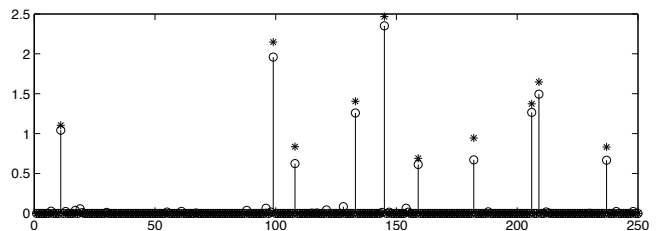
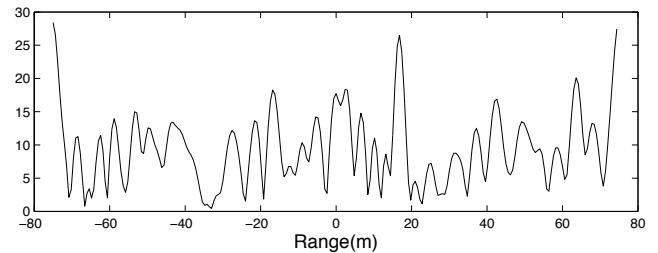


Figure 6: (Top) Received signal for a single carrier transmit LFM waveform and dechirp receiver, (Bottom) Sparse Recovery of target response using BP, \* shows the true target locations and amplitudes,  $\circ$  shows the detected target locations and amplitudes

ers each with 50 Mhz bandwidth with non-overlapping frequency support . The center frequencies and complex phases of the subcarriers are randomly selected at each simulation run. The wideband received waveform is then dechirped using a *single* stretch processor with a single reference chirp of 50 MHz bandwidth and sampled at a rate of 5 Msample/sec of complex I/Q samples corresponding to an unambiguous range of 150 meters. Finally Gaussian complex symmetric noise is added to the samples at the given SNR.

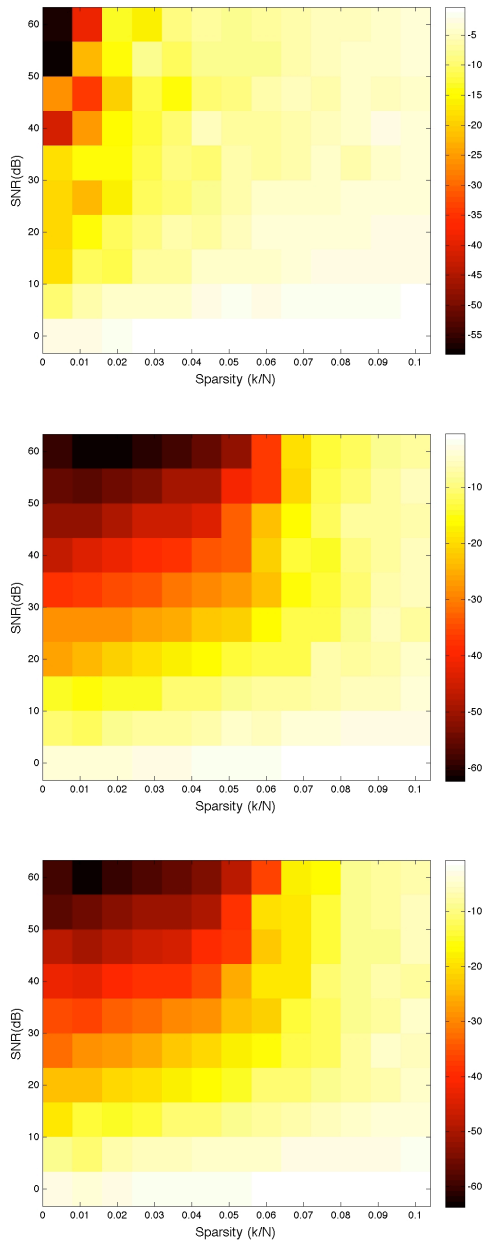


Figure 7: Mean Square Error performance of BP Recovery for  $M = 1, 7, 15$  carriers. for each subfigure x-axis: sparsity( $\delta = K/N$ ) and y-axis: SNR

Figure 5 and 6 shows the results of a single simulation run with 10 point targets of complex amplitude at an SNR level of 20dB for  $M = 1$  and 15 subcarriers. We observe that

for a traditional single carrier chirp system, the system output is readily interpretable as the range profile with resolution matching the 50 MHz bandwidth. Basis pursuit recovery algorithm using the prior knowledge of SNR for the single carrier chirp results in localization of most targets, however closely spaced targets cannot be detected with few false detections. For the multiple carrier chirp transmit waveform the radar receiver output is harder to interpret visually since each of the 10 targets is aliased 15 times. However Basis pursuit recovery algorithm armed with the knowledge of the aliasing pattern can reliably detect all 10 targets.

The results of the Monte Carlo simulations are summarized in Figure 7. We observe that the region of the (SNR, target sparsity) plane where the target response can be estimated with low MSE is larger for multi-carrier chirp waveforms. This is consistent with our observation that multi-carrier chirp waveforms result in lower coherency sensing matrices. We also observe that saturation of the performance as additional subcarriers are added as both the MSE recovery performance and the cumulative coherence distribution are comparable for  $M = 7$  and  $M = 15$ .

## REFERENCES

- [1] E. Candès. The restricted isometry property and its implications for compressed sensing. *Comptes rendus-Mathématique*, 346(9-10):589–592, 2008.
- [2] E. Candès, J. Romberg, and T. Tao. Robust uncertainty principles: Exact signal reconstruction from highly incomplete frequency information. *IEEE Transactions on Information Theory*, 52(2):489–509, 2006.
- [3] D. Donoho. Compressed sensing. *IEEE Transactions on Information Theory*, 52(4):1289–1306, 2006.
- [4] J. Duarte-Carvajalino and G. Sapiro. Learning to sense sparse signals: Simultaneous sensing matrix and sparsifying dictionary optimization. *IEEE Transactions on Image Processing*, 18(7):1395–1408, 2009.
- [5] M. Elad. Optimized projections for compressed sensing. *IEEE Transactions on Signal Processing*, 55(12):5695–5702, 2007.
- [6] E. Ertin. Frequency diverse waveforms for compressive radar sensing. In *2010 International Waveform Diversity and Design Conference (WDD)*, pages 216–219. IEEE, 2010.
- [7] D. T. Gjessing. Matched illumination target adaptive radar for challenging applications. In *Proceedings of IEE Radar Conference*, 1987.
- [8] M. Jankiraman, E. W. De Jong, and P. Van Genderen. Ambiguity analysis of PANDORA multifrequency FMCW/SFCW radar. In *Proceedings of the IEEE International Radar Conference*, pages 35–41, 2000.
- [9] M. Mishali and Y. C. Eldar. Xampling: Analog data compression. In *Proceedings of the Data Compression Conference*, pages 366–375, April 2010.
- [10] M. Skolnik. *Introduction to radar systems*. McGraw-Hill, 1980.
- [11] J. Tropp. Just relax: Convex programming methods for identifying sparse signals in noise. *IEEE Transactions on Information Theory*, 52(3):1030–1051, 2006.